AEDC-TR-74-56

APPLICATION OF A DUAL BEAM LASER VELOCIMETER TO TURBULENT FLOW MEASUREMENTS

V. A. Cline and H. T. Bentley III
ARO, Inc.

ARNOLD ENGINEERING DEVELOPMENT CENTER
AIR FORCE SYSTEMS COMMAND
ARNOLD AIR FORCE STATION, TENNESSEE

September 1974

Final Report for Period July 1, 1972 — June 30, 1973

Prepared for

ARNOLD ENGINEERING DEVELOPMENT CENTER (DYFS)
ARNOLD AIR FORCE STATION, TN 37389

NOTICES

When U. S. Government drawings specifications, or other data are used for any purpose other than a definitely related Government procurement operation, the Government thereby incurs no responsibility nor any obligation whatsoever, and the fact that the Government may have formulated, furnished, or in any way supplied the said drawings, specifications, or other data, is not to be regarded by implication or otherwise, or in any manner licensing the holder or any other person or corporation, or conveying any rights or permission to manufacture, use, or sell any patented invention that may in any way be related thereto.

Qualified users may obtain copies of this report from the Defense Documentation Center.

References to named commercial products in this report are not to be considered in any sense as an endorsement of the product by the United States Air Force or the Government.

APPROVAL STATEMENT

This technical report has been reviewed and is approved.

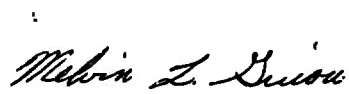

MELVIN L. GUIOU
Captain, USAF
Research and Development
Division
Directorate of Technology

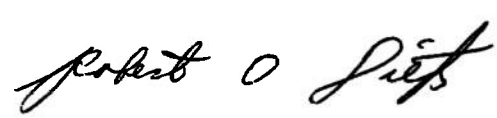

ROBERT O. DIETZ
Director of Technology

UNCLASSIFIED

SECURITY CLASSIFICATION OF THIS PAGE (When Data Entered)

REPORT DOCUMENTATION PAGE		READ INSTRUCTIONS BEFORE COMPLETING FORM
1. REPORT NUMBER AEDC-TR-74-56	2. GOVT ACCESSION NO.	3. RECIPIENT'S CATALOG NUMBER
4. TITLE (and Subtitle) APPLICATION OF A DUAL BEAM LASER VELOCIMETER TO TURBULENT FLOW MEASUREMENTS		5. TYPE OF REPORT & PERIOD COVERED Final Report, July 1, 1972 to June 30, 1973 6. PERFORMING ORG. REPORT NUMBER
7. AUTHOR(s) V. A. Cline and H. T. Bentley III, ARO, Inc.		8. CONTRACT OR GRANT NUMBER(s)
9. PERFORMING ORGANIZATION NAME AND ADDRESS Arnold Engineering Development Center (DY) Arnold Air Force Station, TN 37389		10. PROGRAM ELEMENT, PROJECT, TASK AREA & WORK UNIT NUMBERS Program Element 65802F
11. CONTROLLING OFFICE NAME AND ADDRESS Arnold Engineering Development Center (DYFS), Arnold Air Force Station, TN 37389		12. REPORT DATE September 1974 13. NUMBER OF PAGES 42
14. MONITORING AGENCY NAME & ADDRESS(if different from Controlling Office)		15. SECURITY CLASS. (of this report) UNCLASSIFIED 15a. DECLASSIFICATION/DOWNGRADING SCHEDULE N/A

16. DISTRIBUTION STATEMENT (of this Report)

Approved for public release; distribution unlimited.

17. DISTRIBUTION STATEMENT (of the abstract entered in Block 20, if different from Report)

18. SUPPLEMENTARY NOTES

Available in DDC.

19. KEY WORDS (Continue on reverse side if necessary and identify by block number)

laser velocimetry
turbulence measurements
Doppler effect

20. ABSTRACT (Continue on reverse side if necessary and identify by block number)

A dual beam laser velocimeter (LV) system has been applied to the measurements of mean velocity and turbulence intensity. The basic theory of the LV is described in terms of both Doppler and fringe models. A statistical analysis predicting the number of data points required to ensure a given accuracy is developed. It was found that for a given accuracy and confidence level, significantly larger numbers of data points are required for the turbulent

DD FORM 1 JAN 73 1473 EDITION OF 1 NOV 65 IS OBSOLETE

UNCLASSIFIED

SECURITY CLASSIFICATION OF THIS PAGE (When Data Entered)

20, Continued

intensity than for the mean velocity. Experimental verification of the analysis is given. A theoretical analysis of the LV counting process is proposed which predicts the biases to be found in velocity and turbulent intensity estimators. Of the two most common methods of averaging, the latter yielded, in general, lower biases in the estimators for a one-dimensional model. Finally, experimental LV data are presented, taken from a coaxial free-jet-mixing facility. The LV data are compared with similar pitot probe and hot-wire data with favorable agreement. However, a moderate systematic discrepancy was noted which may be attributed to the LV data reduction technique.

AFSC
Arnold AFS Tenn

PREFACE

The work reported herein was conducted by the Arnold Engineering Development Center (AEDC), Air Force Systems Command (AFSC) under Program Element 65802F. The work was done by ARO, Inc. (a subsidiary of Sverdrup & Parcel and Associates, Inc.), contract operator of AEDC, AFSC, Arnold Air Force Station, Tennessee. The work was performed under ARO Project No. BF382, and the manuscript (ARO Control No. ARO-OMD-TR-74-35) was submitted for publication on April 23, 1974.

The authors wish to thank K. R. Kneile for his help with the statistical accuracy studies, D. O. Barnett for his contribution to the estimator bias analysis, and the personnel of the Engine Test Facility's Fluid Dynamics and Propulsion Group for their cooperation in the use of the jet-mixing facility.

CONTENTS

ILLUSTRATIONS

Figure

1.0 INTRODUCTION

The purpose of this report is to describe the results of studies to investigate the application of standard laser velocimeter (LV) techniques for measurements in turbulent flows. Turbulence is characterized by the excursions of the instantaneous velocity at a point about a mean flow velocity. Both the frequency and the magnitude of these excursions are of interest to the aerodynamicist. Studies are under way by several organizations (Refs. 1, 2, and 3) involving LV measurements of the power spectral density, shear stress, and other parameters. The scope of this project has been limited to measuring the magnitude of the turbulence, the turbulent intensity.

The traditional aerodynamic diagnostic tools such as the pitot probe are well suited with their time-averaging aspects for the measurement of the average or mean velocity, but only the hot-wire anemometer has been successful in measuring turbulence parameters. The hot wire provides an indirect measurement of turbulence by analyzing the heat-transfer rate of the wire as affected by convective cooling. It is extremely delicate, requiring extreme care in use and tedious calibration procedures. The LV offers many advantages over the hot wire. It is nonperturbing to the flow of interest, and it is unaffected by harsh environments such as extreme heat. It offers very good spatial resolution with typical probe volumes as small as 2×10^{-5} cm^3 and allows close proximity to models of interest for boundary-layer studies, etc. Its outstanding point in this study is the inherent similarity of the LV method to the parameter of interest. The LV makes many individual "instantaneous" determinations of velocity from which a mean velocity is found. Thus, the mean velocity and the magnitude of the excursions about the mean are directly measured by the LV.

The studies conducted under this program were intended to provide insight into known problem areas concerning LV applications and to uncover and define other problems through the reduction of typical LV data to find the turbulent intensity. Data reduction techniques were studied in depth. A comparison of experimental and analytical determinations of accuracy versus sample size is presented for mean velocity and turbulent intensity. It is hoped that direction is provided for implementation of the LV technique to reliable turbulence measurements.

2.0 THE LV TECHNIQUE

The LV technique is based on the Doppler frequency shift of radiation emitted or scattered from a moving source.

The shift (or difference) in frequency between radiation incident on a moving particle and the radiation received after being reflected or scattered from that particle is expressed as

$$f_d = f_s - f_o = \frac{n\vec{v}}{\lambda_o} \cdot (\hat{e}_s - \hat{e}_i) \tag{2.1}$$

where

f_d = Doppler frequency shift
f_s = frequency of scattered radiation
f_o = frequency of incident radiation
n = index of refraction of the medium
$\vec{v}$ = scatter source velocity vector
λ_o = free-space wavelength of the incident radiation
$\hat{e}_s$ = unit vector in the direction of scatter
$\hat{e}_i$ = unit vector in the direction of incident radiation

Equation (2.1), derived in Ref. 4, shows that the measurable frequency difference is dependent on the scatter source velocity and the directions of incident and scattered radiation. In practice, it is convenient to use a particular geometric configuration referred to as a "dual scatter" system, in which two incident beams of radiation are simultaneously scattered from the same particle in a common direction, $\hat{e}_S$ (Fig. 1). From Eq. (2.1) the radiation scattered from the first beam is

$$f_{s_1} = f_o + \frac{n\vec{v}}{\lambda_o} \cdot (\hat{e}_s - \hat{e}_{i_1}) \tag{2.2}$$

Similarly,

$$f_{s_2} = f_o + \frac{n\vec{v}}{\lambda_o} \cdot (\hat{e}_s - \hat{e}_{i_2}) \tag{2.3}$$

The frequency difference, measurable by the optical heterodyning technique, is then

$$f_{s_1} - f_{s_2} = f_d = \frac{n\vec{v}}{\lambda_o} \cdot (\hat{e}_{i_2} - \hat{e}_{i_1}) \tag{2.4}$$

The measured frequency difference is now independent of the direction of observation ($\hat{e}_S$), which gives great versatility to this arrangement. Further convenience is added in the form

$$f_d = \frac{2 \sin \theta/2}{\lambda_o} \vec{nv} \cdot \hat{e}_\perp \qquad (2.5)$$

where θ is the angle between the two incident beams and $\hat{e}_\perp$ is the unit vector perpendicular to the mean illuminating direction. The angle θ can be measured quite precisely, thus allowing an accurate direct measurement of scatter source velocity.

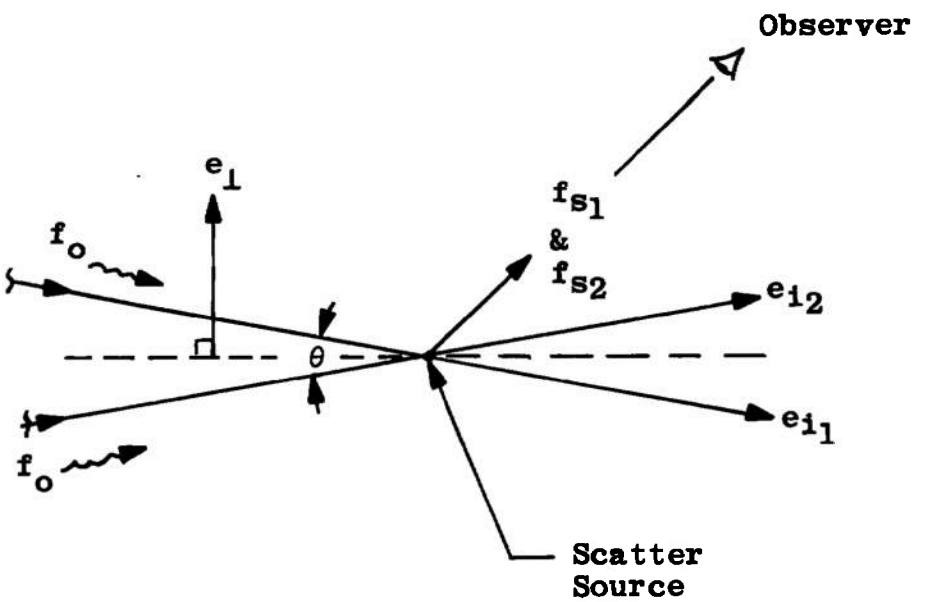

Figure 1. Dual scatter technique.

The same results are obtained, but more insight into the physical mechanism is acquired by looking at the spatial interference pattern from the two coherent illuminating beams of the dual scatter system. A set of bright and dark fringes is set up where the two incident beams cross, as shown in Fig. 2. The input waves are indicated by lines representing the high intensity crests one wavelength apart. Constructive interference of the two produces the fringes, bright where the two wave crests are superimposed, and dark at the superposition of a crest and a trough. The spacing between fringes is seen to be

$$\delta = \frac{\lambda}{2 \sin \theta/2}$$

A particle moving across the fringe pattern will scatter light with intensity varying as the fringe pattern intensity and with a frequency directly proportional to the component of its velocity normal to the fringes. The period of this a-c signal is the time required to travel a known distance (the fringe spacing). Fundamentally, velocity equals distance divided by time, or

$$\vec{v} \cdot \hat{e}_n = \frac{\lambda}{2 \sin \theta/2} \times \frac{1}{\tau} \tag{2.6}$$

or as before, since the signal frequency (f) equals $1/\tau$ and the wavelength in a medium of index of refraction n is λ_o/n, then

$$f = \frac{2 \sin \theta/2}{\lambda_o} n\vec{v} \cdot \hat{e}_n \tag{2.7}$$

where $\hat{e}_n$ is a unit vector normal to the fringes. It is obvious from Fig. 2 that $\hat{e}_n = \hat{e}_\perp$.

Many arrangements using this basic method are possible. A typical dual scatter system is schematically shown in Fig. 3. A signal burst of velocity information is received each time a scattering source passes through the fringe region. Eight cycles are used to determine the period of the signal by the Data Processor (DP) developed at AEDC (Refs. 4 and 5). A collection of these "instantaneous" measurements is used to statistically determine the parameters of interest.

"Instantaneous" indicates a short measurement time with respect to the flow velocity variation of interest (i. e., the turbulent frequency). A typical LV, measuring a 100 ft/sec flow velocity, would have a signal frequency of about 2 MHz, the period of which is 0.5 μsec. Since eight cycles are used to measure the velocity, the measurement time is 4 μsec. Assuming an order of magnitude difference between measurement time and the period of the turbulent frequency, the measurement could be considered instantaneous with respect to a turbulent frequency of one cycle in 40 μsec, or 25 KHz.

Investigations involving shear stress measurements (Ref. 6) indicated that the major contributions corresponded to frequencies below 5 KHz; therefore, the LV measurements are instantaneous in many flows of interest.

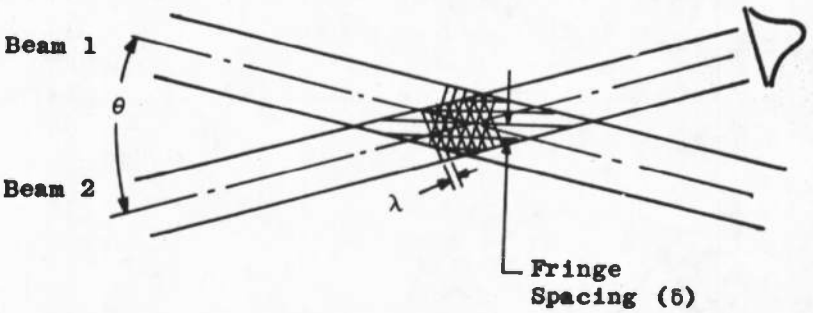

a. Beam crossover region

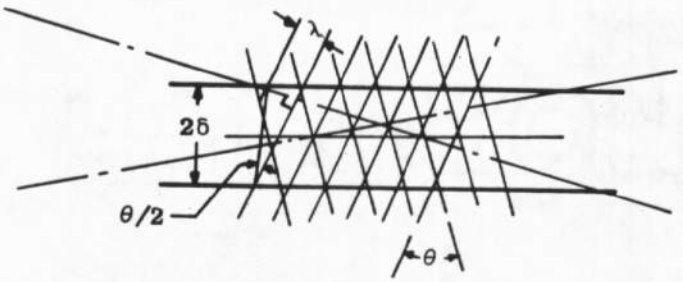

b. Enlargement of interference region

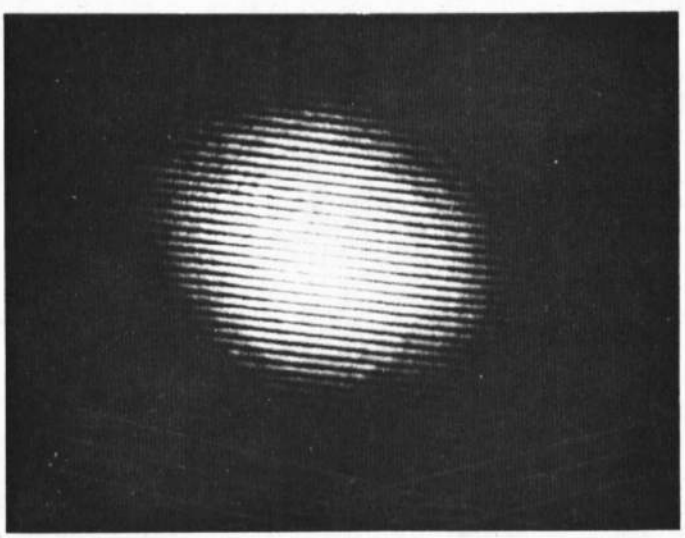

c. Photo of actual fringe pattern

Figure 2. Dual scatter interferences fringes.

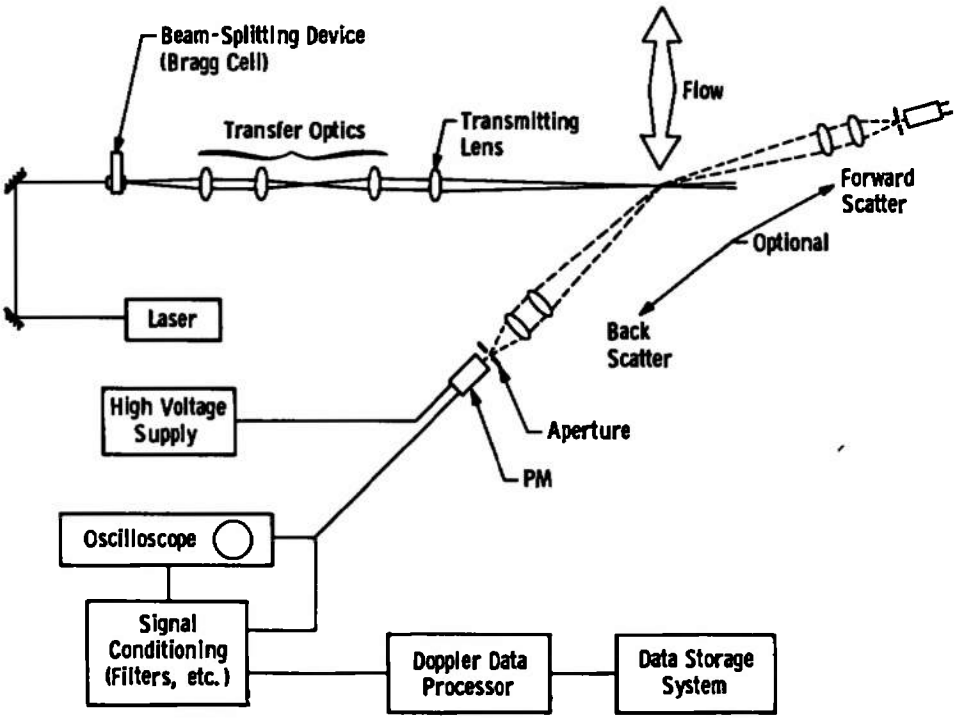

Figure 3. Typical dual scatter system.

3.0 STATISTICS

The values of the flow parameters determined with the LV are the results of statistical analysis of a collection of individual measurements. Immediately in question is the number of data points necessary to ensure a given accuracy of the parameter of interest. Typically, estimates of the required number of data points have been made from approximation formulas based on the assumption of a normal distribution (Ref. 7). An analysis not predicated upon this assumption was made, and the results were then compared with values obtained from actual experimental LV data.

Consider a one-dimensional flow having an infinite population of velocities distributed about the mean velocity, μ, with standard deviation σ, from which the turbulent intensity (TI) = σ/μ can be defined. The accuracy to which the true values, μ and TI, are approximated by the values $\bar{v}$ and $s/\bar{v}$ from a smaller sample is desired. Stated another way, the question is asked, what are the variance of the mean value ($\bar{v}$) and the variance of the standard deviation (s) of many smaller samples of size N?

We are interested in specifying a maximum tolerance on the mean velocity measurement and on the turbulent intensity. Equations for the statistical analysis were taken from Ref. 7, Chapter 4. Let the sample mean be indicated by $\bar{v}$. The variance of the mean of a sample of N measurements ($\sigma^2_{\bar{v}}$) is related to the population variance (σ^2) by

$$\sigma^2_{\bar{v}} = \sigma^2/N \tag{3.1}$$

The relationship of the standard deviations is then

$$\sigma_{\bar{v}} = \sigma/\sqrt{N} \tag{3.2}$$

A tolerance on the mean value of a single sample ($\bar{v}$) can be defined as a number (Z) of standard deviations of the mean ($\sigma_{\bar{v}}$) divided by the true (population) mean value.

$$\text{Tol.}(\bar{v}) = \frac{Z\,\sigma_{\bar{v}}}{\mu} \tag{3.3}$$

The Z defines the confidence level of the measurement. For example, a 68-percent probability exists that a single measurement will fall within 1σ of the mean (Z = 1). Z = 2 and 3 provide 95-percent probability of less than 2σ, and 98-percent probability of less than 3σ deviation from the mean, respectively. Relating to the population parameters, then

$$\text{Tol.}(\bar{v}) = \frac{Z\sigma}{\sqrt{N}\,\mu} \tag{3.4}$$

and since the turbulent intensity (TI) is the standard deviation of the population divided by the mean, then

$$\text{Tol.}(\bar{v}) = \frac{Z(TI)}{\sqrt{N}}$$

It is seen that the tolerance on the sample mean velocity is dependent on the population turbulent intensity.

For the determination of tolerance of the turbulent intensity we introduce the rel-variance of a parameter (x), which is defined as

$$V^2_x = \frac{\sigma^2_x}{\bar{x}^2} \tag{3.5}$$

where σ_x^2 (the square of the standard deviation) is the variance of x, and $\bar{x}$ is the mean value or expected value.

Letting s represent the sample standard deviation, the rel-variance of the estimated variance for a simple random sample is

$$V_{s^2}^2 = \frac{1}{N}\left(\beta - \frac{N-3}{N-1}\right) \tag{3.6}$$

For large N

$$V_{s^2}^2 \cong \frac{\beta - 1}{N} \tag{3.7}$$

β is called the kurtosis of the distribution and is defined as

$$\beta = \frac{\mu_4}{\sigma^4}$$

where $\mu_4 = \epsilon\,[(v_i - \mu)^4]$ is the expected value of the fourth moment about the mean and $\sigma^2 = \epsilon[(v_i - \mu)^2]$ is the expected value of the second moment of v. The value of kurtosis is always three for a Gaussian distribution.

The rel-variance of the estimated standard deviation is given by the approximation

$$V_s^2 \cong 1/4\, V_{s^2}^2 \tag{3.8}$$

The equation will give good results for moderately large values of N where

$$V_{s^2} \cong \sqrt{\frac{\beta - 1}{N}} < 0.3$$

Using Eq. (3.7),

$$V_s^2 \cong \frac{\beta - 1}{4N} \tag{3.9}$$

The rel-variance of the ratio of two random variables, as in the case of the measured turbulent intensity $(s/\bar{v})$ is, neglecting correlation terms,

$$V^2_{(s/\bar{v})} \cong V^2_s + V^2_{\bar{v}}$$

$$\cong \frac{\beta - 1}{4N} + \frac{\sigma^2_{\bar{v}}}{\mu^2}$$

$$\cong \frac{\beta - 1}{4N} + \frac{\sigma^2}{N\mu^2} \tag{3.10}$$

or, in terms of the relative turbulent intensity,

$$V^2_{(s/\bar{v})} = \frac{1}{N}\left[\frac{\beta - 1}{4} + (TI)^2\right] \tag{3.11}$$

The omission of the correlation term in Eq. (3.10) was experimentally justified as seen below by the good agreement with experiment. In general, if the distribution is near normal, the correlation term is small, and in no case would the discrepancy be more than $\pm V^2_{(s/\bar{v})}$.

We define the tolerance of the turbulent intensity as

$$\text{Tol. (TI)} = \frac{\text{Z Sample Std. Deviations of (TI)}}{\text{Expected Value of (TI)}}$$

which is by definition $ZV_{(s/\bar{v})}$ or, finally,

$$\text{Tol. (TI)} = Z\sqrt{\frac{1}{N}\left[\frac{\beta - 1}{4} + (TI)^2\right]} \tag{3.12}$$

It is seen that the accuracy of the measurement of both the mean velocity and the turbulent intensity is dependent on the level of turbulence in the flow. Figure 4 shows the sample size required to ensure a given tolerance on mean velocity for five values of TI. A similar plot for turbulent intensity is seen in Fig. 5, assuming a normally distributed population (kurtosis = 3).

An experiment was set up to ascertain the validity of the analytical results. A single component, dual scatter LV was used to measure velocities in a low-speed V/STOL wind tunnel. A turbulence generator was placed in the flow to give a moderate turbulence level which was found to be 12 percent upon data reduction. A large number of data points (10,000) which would theoretically assure (with 95-percent confidence) a 2-percent accuracy on TI for a 10-percent turbulence level,

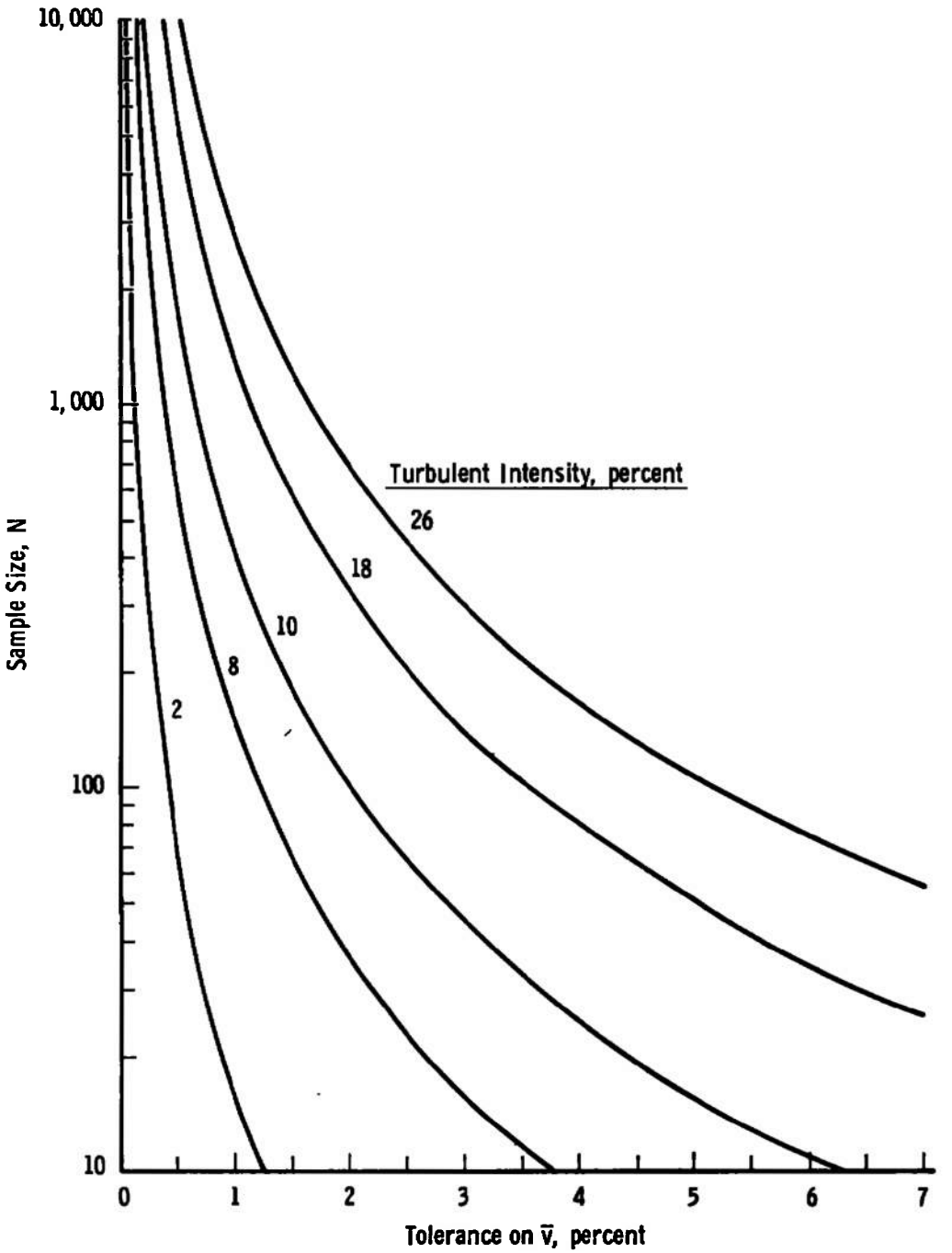

Figure 4. Tolerance on mean velocity versus sample size for 2σ confidence level.

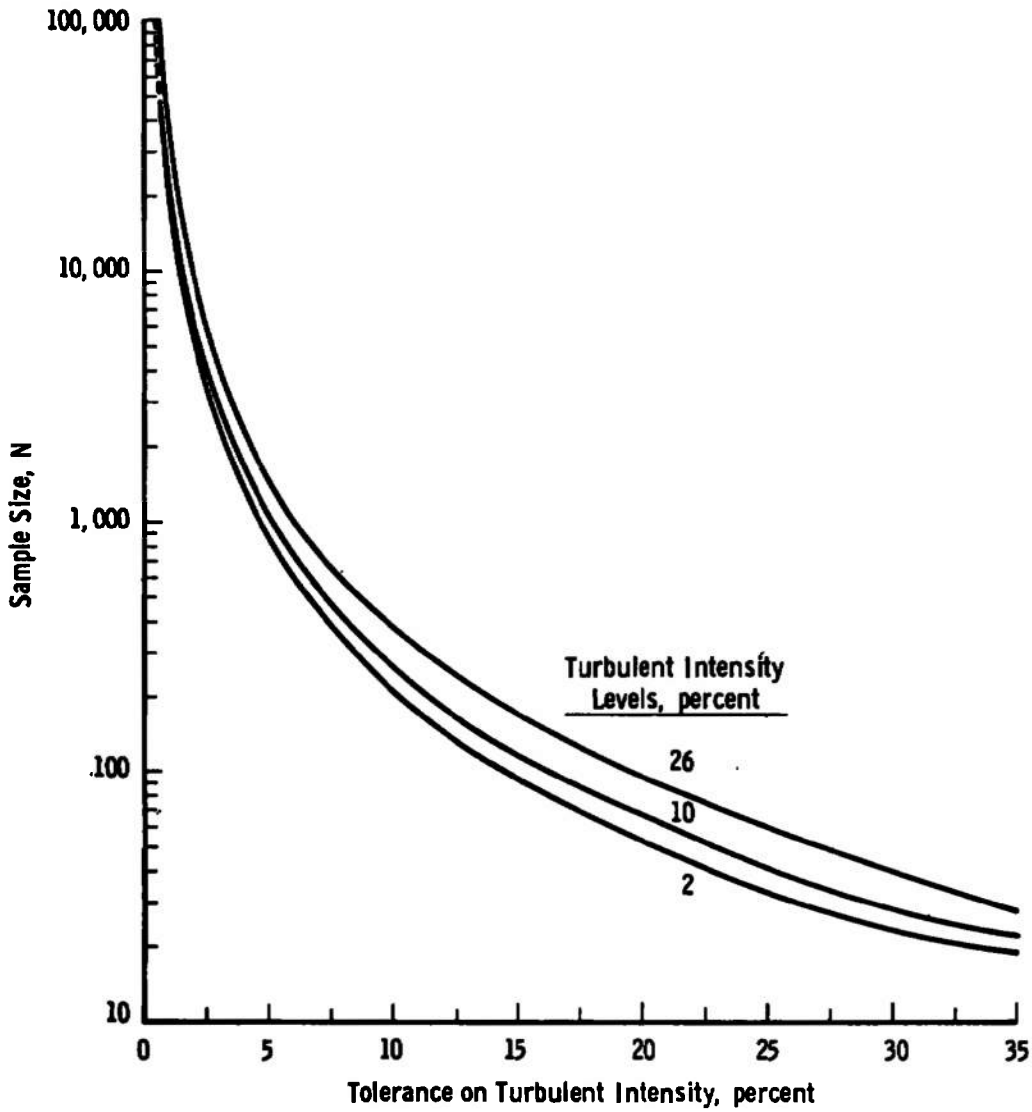

Figure 5. Tolerance on turbulent intensity versus sample size for 2σ confidence level.

were taken at one position in the flow. A histogram of the collection showing number of data points per velocity increment of 1 ft/sec is seen in Fig. 6. From this population, 100 samples with N number of data points were selected for several values of N, using simple random sampling with replacement. The random sampling was used to negate any low frequency velocity variations which might have been caused by a slight drift in tunnel conditions during data collection.

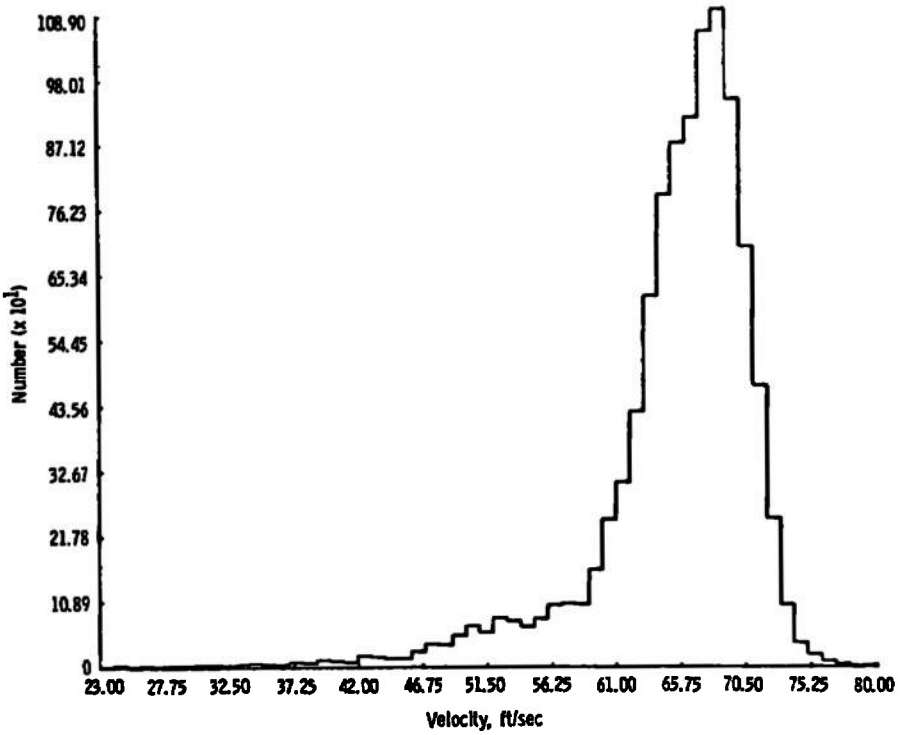

Figure 6. Velocity distribution, N = 10,000.

For each sample of N points, the mean velocity and the turbulent intensity were calculated. This produced 100 values of $\bar{v}$ and TI. The standard deviation of these 100 values is a measure of the accuracy one could expect by taking a single sample of size N. To parallel the analytical study the tolerance was defined to be two standard deviations of the parameter divided by the mean value based on all 10,000 data points. This gives 95-percent confidence in the measurement.

$$\text{Tol.}\,(\bar{v}) = \frac{2\sigma_{\bar{v}}}{\mu} \qquad \text{Tol.}\,(\text{TI}) = \frac{2\sigma_{\text{TI}}}{\sigma/\mu}$$

The comparison of the experimental and analytical values was extremely good for mean velocity, as seen in Fig. 7.

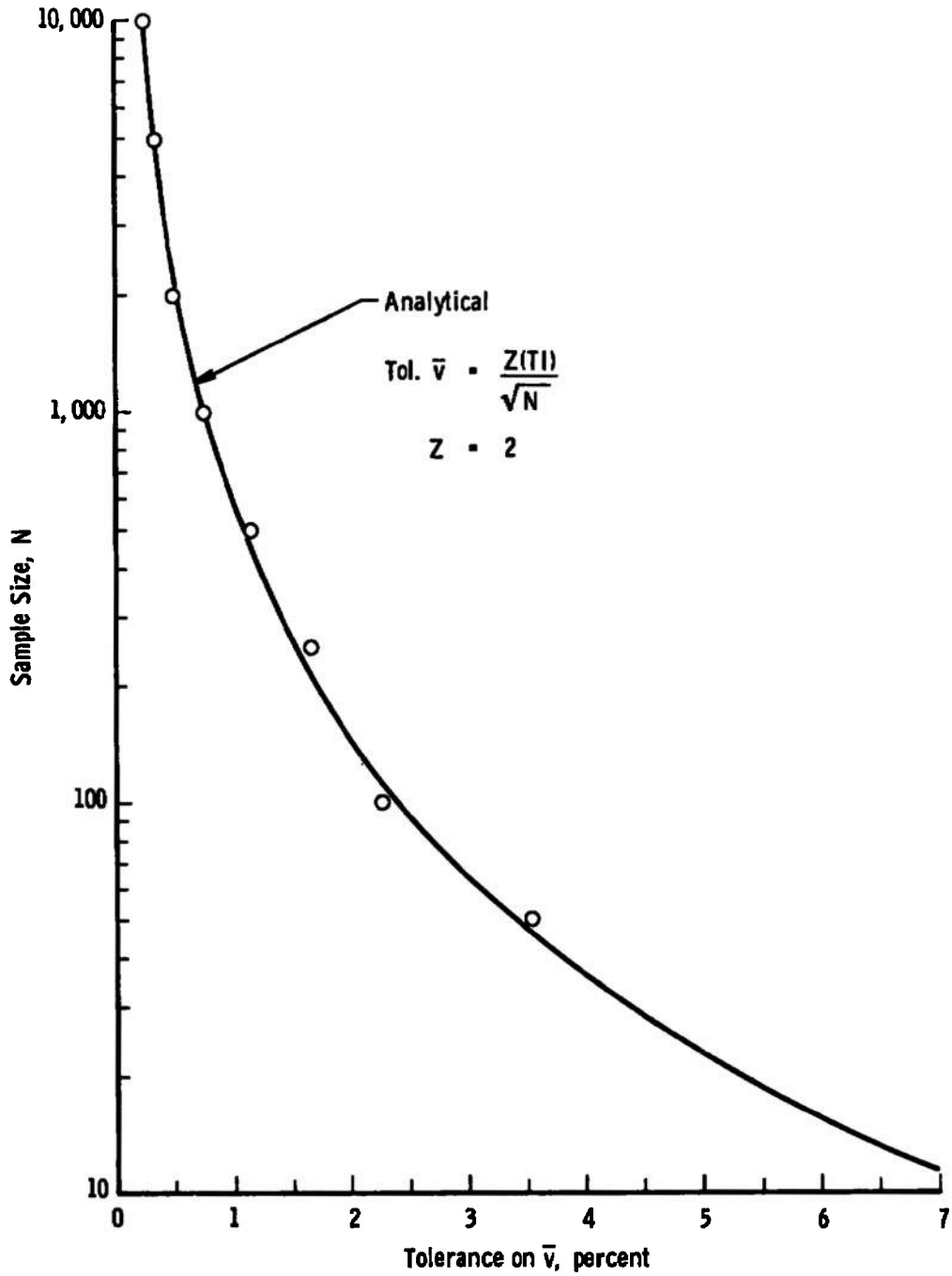

Figure 7. Tolerance on mean velocity experiment versus theory for turbulent intensity = 12 percent.

The comparison of the turbulent intensity data was very poor assuming a normal distribution ($\beta = 3$). The kurtosis was calculated for the distribution and found to be 40.3. With $\beta = 40$, the analytical values and the experimental data compared well, as seen in Figure 8. For $\beta = 40$ the analytical approximations used are good for N values greater than 433.

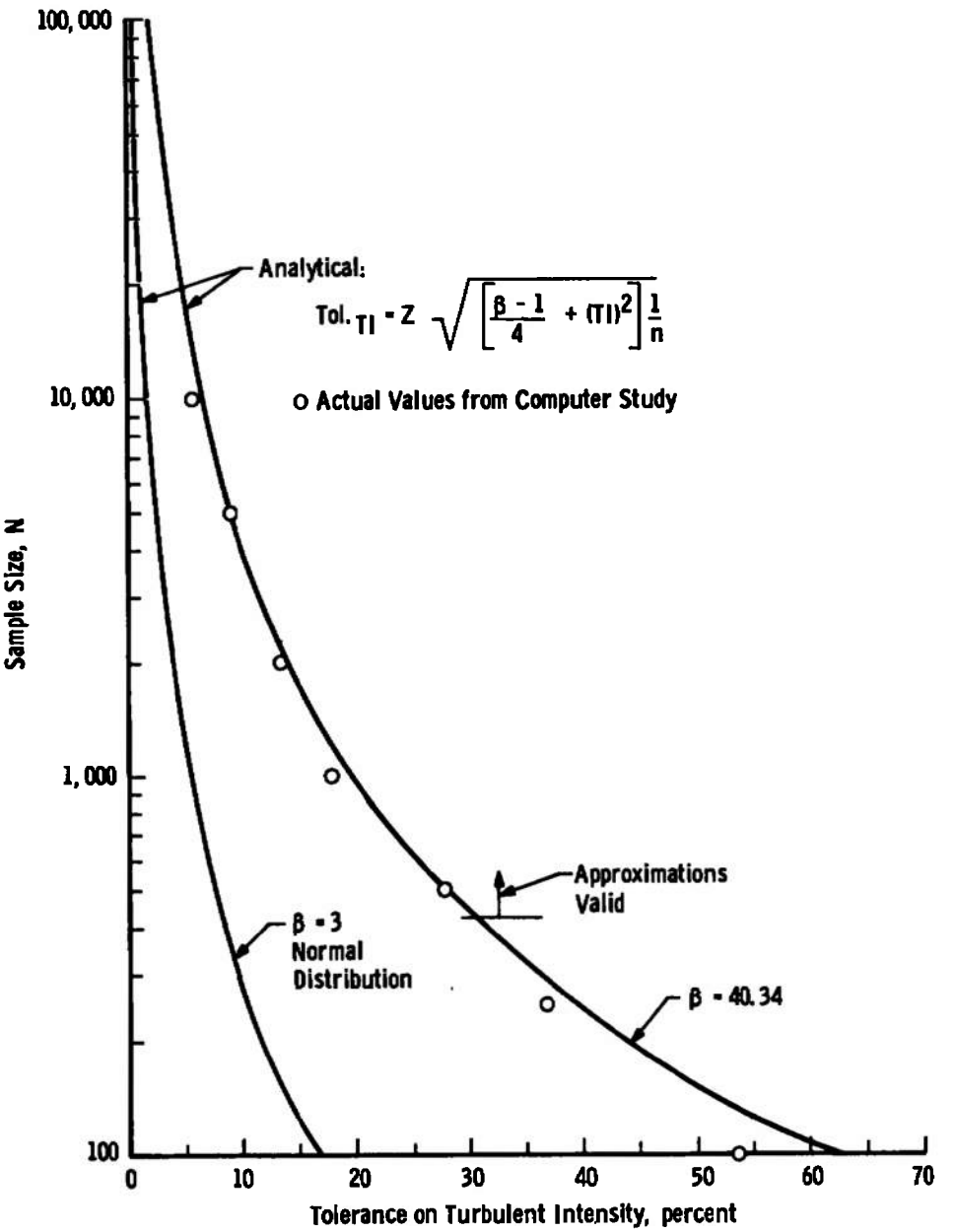

Figure 8. Tolerance on measurement of turbulent intensity versus sample size for TI = 12 percent and 2σ confidence level.

The impact of this is that for this set of data from a typical dual scatter LV, an order of magnitude increase in the number of data points is required to assure the same accuracy on TI that one would expect for a normal distribution.

An important question is whether the kurtosis value can be influenced by the turbulence source, turbulence level, and other flow characteristics. The answer is yes, and it was also seen to reach extreme values. To verify this conclusion, a second collection of 10,000 data points was taken in the free stream of the V/STOL wind tunnel (Fig. 9). The turbulent intensity calculated from this collection was found to be 3.1 percent. The kurtosis value was found to be 1,533. The analytical prediction using this value is shown with the values experimentally obtained from the population in Fig. 10. Again, good agreement is seen for large values of N where the approximation formulas are valid. Of course, the tolerance values greater than 100 percent are only for those values of turbulent intensity greater than actual. The disturbing prospect of a widely varying kurtosis indicates that in an unknown turbulent flow, an accuracy versus sample size prediction cannot be made prior to data acquisition.

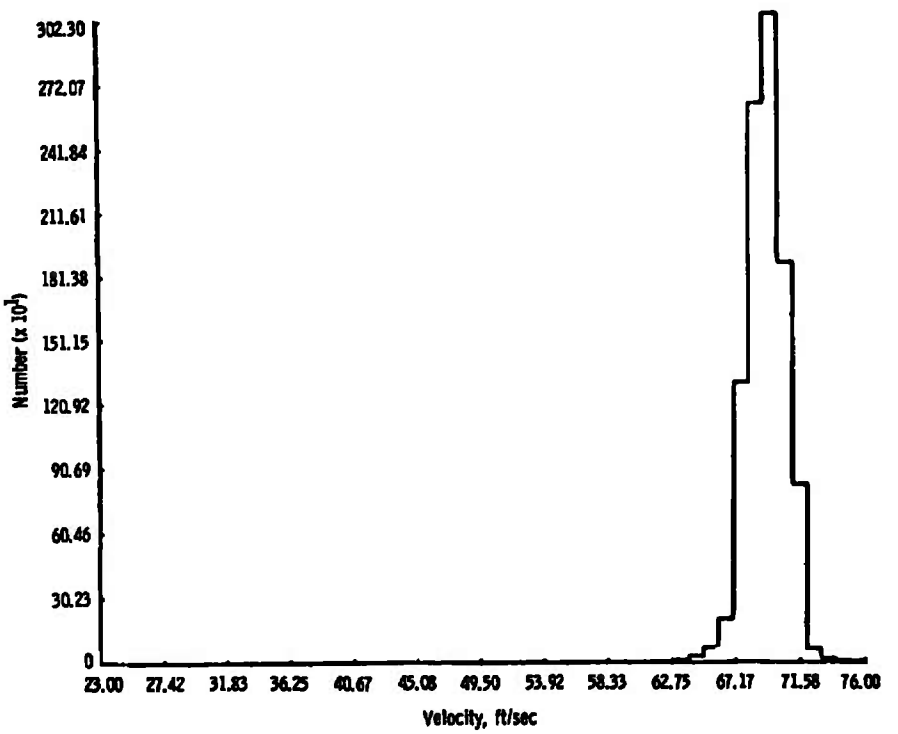

Figure 9. Free-stream velocity distribution, N = 10,000.

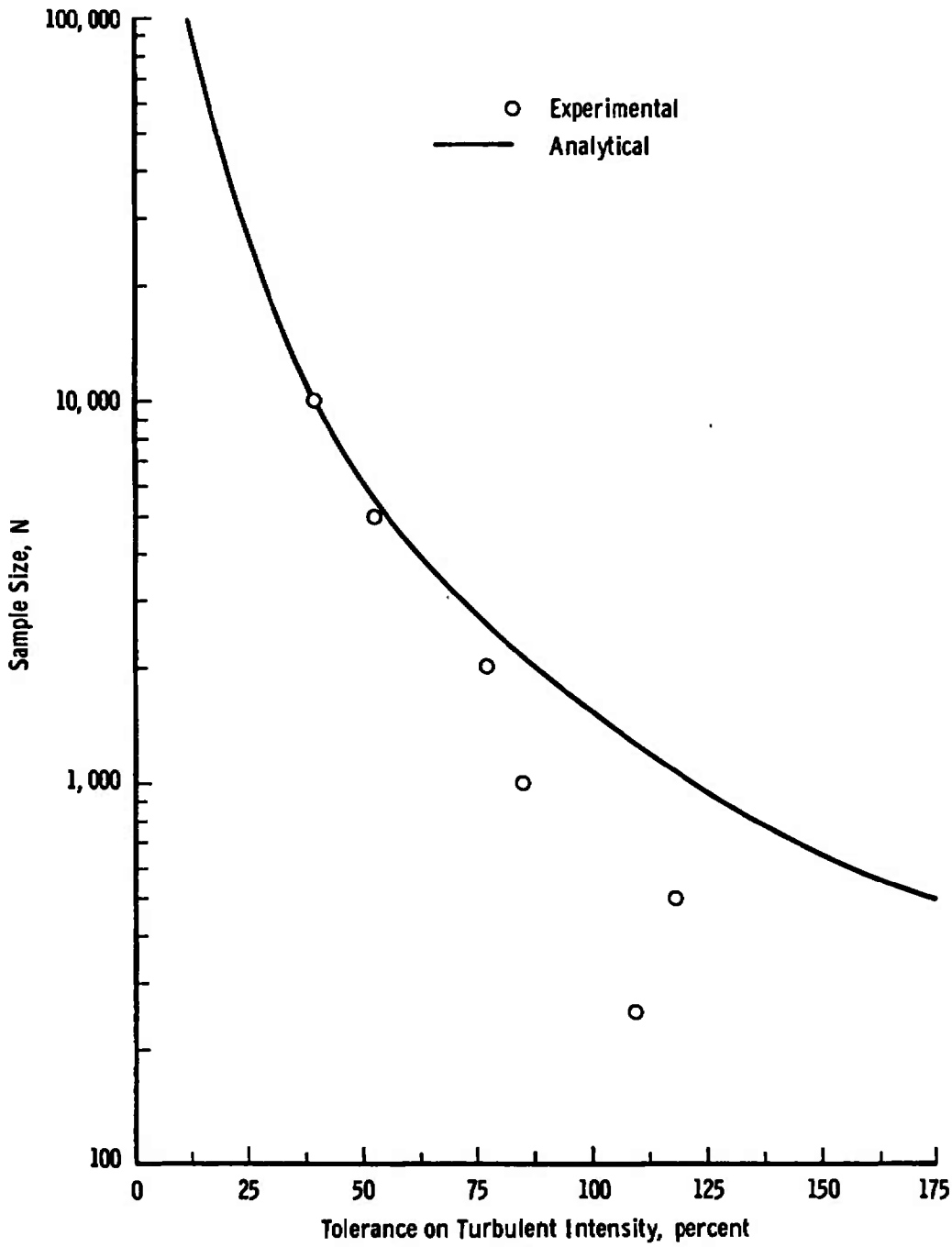

Figure 10. Sample size versus tolerance on turbulent intensity for 2σ confidence level, TI = 3 percent.

Laser velocimeter turbulent intensity measurements in a fully developed channel flow with relative turbulent intensities between 4 and 6 percent are reported in Ref. 8. It is shown there that a slight variation of kurtosis (labeled flatness factor) existed through the flow profile, but it was always near the value of 3, corresponding to a normal

distribution. It is believed that the significant difference in the two experiments is that many of the large particles were filtered out of the flow in the Naval Ordinance Laboratory (NOL) study, indicating that particle dynamics may be the primary cause for the kurtosis variation. Also, Chauvenet's criterion, which neglects all data over 2σ from the mean, was used in the reduction of the NOL data, where no data were rejected in the present case. Data rejection is a source of debate, and of course the two factors are tied together in that most of the data points rejected may be from large particles lagging the flow. It is fair to assume then that for some experimental configurations (where sufficient flow filtering is possible) the problem may be attacked at the data acquisition end, giving a reasonable number of data points required. Further study of the distribution shape factor is in order.

It is important to emphasize that the discussion is concerned with probabilities and tolerances and not actual error magnitudes occurring with a given sample size. It can only be stated that 95 times out of 100 the values obtained from a single statistical sample of size N will fall within the 2σ limit. Indeed, 68 percent of the time, the value will fall within half that limit, and of course the most probable value is the mode, or peak, value.

4.0 DATA ANALYSIS

The raw data output of the LV is in terms of the period (τ) of the Doppler signal. The desired parameters are in terms of frequency, or $1/\tau$. Two methods of reducing LV data have typically been used. One method is to find the mean period of a collection of data and from that to calculate the parameters. The other is to convert each period measured to a frequency and then carry out the statistical manipulations on frequencies. Basic considerations would say that if one were interested in velocity

$$v = K \times \frac{1}{\tau \pm \Delta\tau}$$

and if the measurement error ($\Delta\tau$) of the period was small, then frequency averaging would be the proper way for an unbiased estimator. However, consider the following. For a counting-type LV, the rate at which scatter centers enter the probe volume is dependent on the particle density [n(t)], the velocity [v(t)], and the effective sampling area, A; i.e.,

$$\dot{N} = n|v|A \qquad (4.1)$$

The symbol N, representing particle flux, should not be confused with sample size from the preceding section. The absolute value sign can be removed if the flow is in one direction only. It is obvious that in a burst-type situation (i.e., where the data are not continuous) a collection of data would be weighted toward the higher velocities in a turbulent flow. This is a biasing effect on both the mean velocity and the turbulent intensity. An analysis of this biasing is presented for the case of one-dimensional turbulent flow.

The LV is assumed to be operating in the regime where the individual measured velocities are constant during the probe volume transit time. That is, the turbulent eddies are much larger than the probe volume size. This ensures that each particle transit produces only one velocity measurement. As individual velocity readings in turbulent flow have little meaning taken singly, average quantities are therefore taken.

A further restriction must now be imposed. The following analysis is based on the assumption that the count rate is totally determined by the particle arrival rate in the probe volume. This is true only for the case where

$$\dot{N} > \frac{1}{t_r}$$

where t_r is the system dead time. The net result of large dead times is to reduce the bias for certain variable estimators. The analysis which follows will set limits on the biases which can be expected from an individual realization LV system.

If Q is some well behaved function of velocity, then the measured average of the quantity $\overline{Q}_m$ is given by

$$\overline{Q}_m = \frac{\langle \dot{N} Q \rangle}{\langle N \rangle} \tag{4.2}$$

where

$$\langle\ \rangle \equiv \frac{1}{T} \int_0^T dt \Big|_{\lim T \to \infty}$$

Due to the discrete nature of the counting process this is true only for large numbers of particle events and when the sample rate is high with respect to the velocity fluctuations of interest. For a more detailed discussion of the validity of the assumptions inherent in Eq. (4.2) the reader is referred to Appendix A by D. O. Barnett and Ref. 9. To determine the number of events required to assert that the mean velocity

is accurate to within a predetermined accuracy, the analysis of Section 3.0 is used. Frequency averaging refers to the arithmetic averaging of the periods first converted to frequency. The set of frequency samples, $\{f_1, \ldots f_N\}$, is related to the set of period samples, $\{T_1, \ldots T_N\}$ by the equation

$$V_i = \frac{K}{T_i} = Kf_i \tag{4.3}$$

The measured mean velocity as computed by the two methods will now be derived. The results will be given in terms of the actual flow parameters, mean velocity and turbulent intensity.

For both cases, period and frequency averaging, the number density of countable particles will be assumed to consist of a mean value, $\bar{n}$, and a time-fluctuating component, n', such that

$$\langle n \rangle = \langle \bar{n} + n' \rangle = \bar{n} \tag{4.4}$$

Similarly for the velocity,

$$\langle v \rangle = \langle \bar{v} + v' \rangle = \bar{v} \tag{4.5}$$

4.1 MEASURES OF THE MEAN VELOCITY

When a variable appears subscripted by m, followed by T or f, the quantity is a measured estimator of that variable averaged by period or frequency, respectively. For example, $\bar{v}_{mf}$ is a velocity estimator obtained by frequency averaging. From the count rate model previously introduced, the measured frequency-averaged mean velocity in terms of flow parameters is

$$\bar{v}_{mf} = K\bar{f} = \frac{k\langle nvf \rangle}{\langle nv \rangle} = \frac{\langle nv^2 \rangle}{\langle nv \rangle} \tag{4.6}$$

Upon substitution for the number density and velocity relationships, Eqs. (4.4) and (4.5), and keeping only second-order terms, Eq. (4.6) becomes

$$\bar{v}_{mf} = \bar{v}\left(\frac{1 + \dfrac{\langle v'^2 \rangle}{\bar{v}^2} + 2\dfrac{\langle n'v' \rangle}{\bar{n}\,\bar{v}}}{1 + \dfrac{\langle n'v' \rangle}{\bar{n}\,\bar{v}}}\right) \tag{4.7}$$

A plot of the percentage error as a function of the correlation is shown in Fig. 11. Assuming that n′ is independent of v′, Eq. (4.7) may be written as

$$\bar{v}_{mf} = \bar{v}\left(1 + \frac{\langle v'^2 \rangle}{\bar{v}^2}\right) \tag{4.8}$$

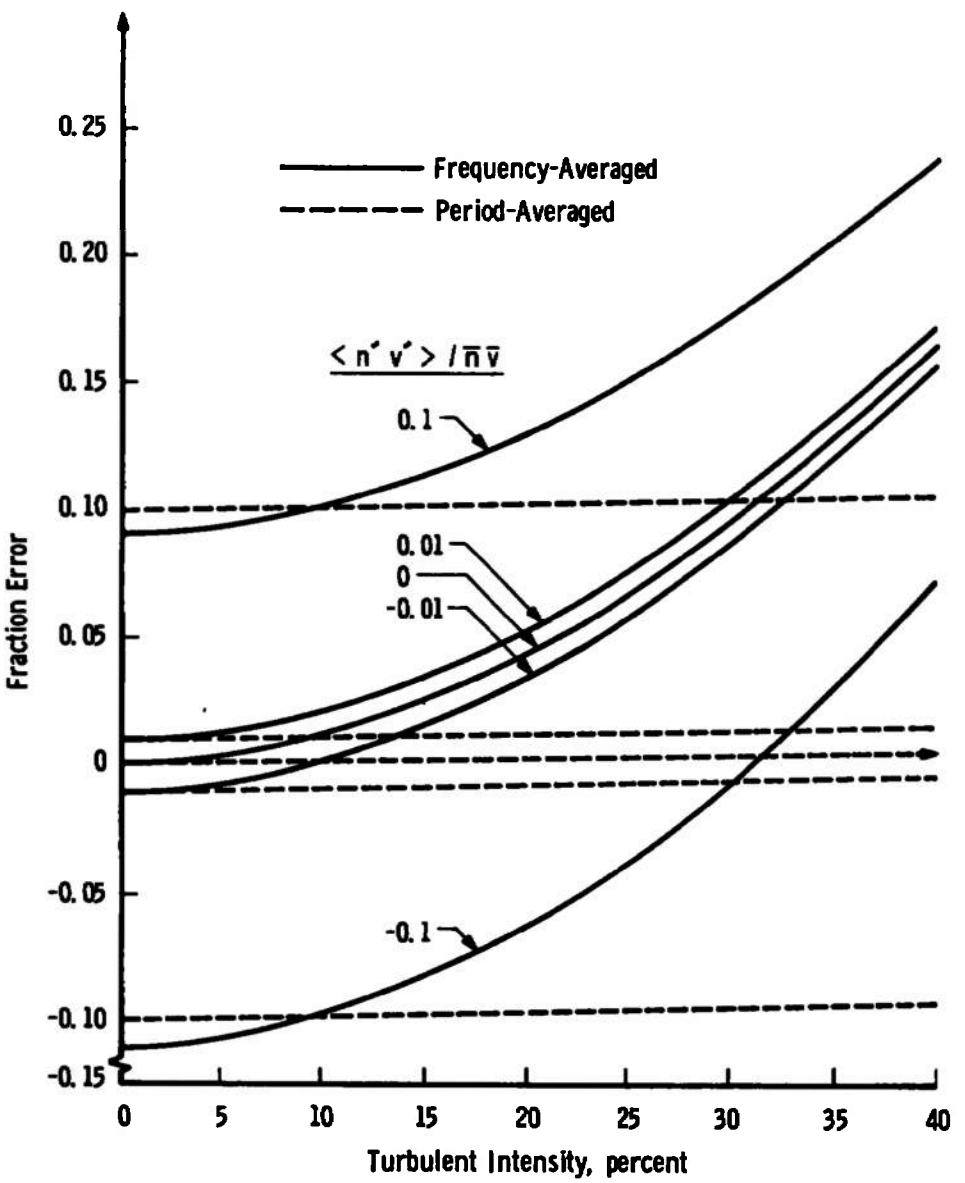

Figure 11. Fraction error in measured velocities.

This assumption is not generally valid. For example, a mixing region will show a large correlation if the sources have different particle concentrations. The term $\langle v'^2 \rangle / \bar{v}^2$ is just the square of the actual turbulent intensity. This constitutes a biasing of the calculated mean toward higher velocities, which can be significant for high turbulent intensities. The left-hand side of Eq. (4.7), and consequently that of Eq. (4.8), are the measureable quantities. The remaining terms are yet-unknown flow parameters.

The period-averaged velocity in terms of flow parameters is

$$\bar{v}_{mT} \triangleq \frac{K}{\bar{T}} = K \frac{\langle n\, v \rangle}{\langle nvT \rangle} = \frac{\langle nv \rangle}{\langle n \rangle} = \bar{v}\left(1 - \frac{\langle n'v' \rangle}{\bar{n}\,\bar{v}}\right) \tag{4.9}$$

Again assuming the independence of n' and v', one finds the bracketed term is unity. The velocity calculated from the periods is found to accurately measure the true mean velocity of the flow independent of the turbulent intensity.

4.2 MEASURES OF THE TURBULENT INTENSITY

The turbulent intensity, as it would be measured by the LV, can also be calculated in terms of the flow parameters. The frequency-averaged turbulent intensity is given by

$$\overline{(TI)^2_{mf}} = \frac{\langle v'^2 \rangle_{mf}}{\bar{v}^2_{mf}} = \frac{\langle \dot{N}(v - \bar{v}_{mf})^2 \rangle}{\langle \dot{N} \rangle \bar{v}^2_{mf}} = \frac{\langle \dot{N} v^2 \rangle}{\langle \dot{N} \rangle \bar{v}^2_{mf}} - 1 \tag{4.10}$$

The measured velocity must be used since the true velocity is unknown.

Upon substituting for n and v as before and neglecting all terms greater than second order, one arrives at

$$\overline{(TI)^2_{mf}} \cong \frac{\dfrac{\langle v'^2 \rangle}{\bar{v}^2}\left(1 - \dfrac{\langle v'^2 \rangle}{\bar{v}^2} - \dfrac{\langle n'v' \rangle}{\bar{n}\,\bar{v}}\right) - \dfrac{\langle n'v' \rangle}{\bar{n}\,\bar{v}}}{1 + \dfrac{\langle v'^2 \rangle}{\bar{v}^2}\left(2 + \dfrac{\langle v'^2 \rangle}{\bar{v}^2} + 4\dfrac{\langle n'v' \rangle}{\bar{n}\,\bar{v}}\right) + 4\dfrac{\langle n'v' \rangle}{\bar{n}\,\bar{v}}\left(1 + \dfrac{\langle n'v' \rangle}{\bar{n}\,\bar{v}}\right)} \tag{4.11}$$

The previously calculated value for the measured frequency-averaged velocity, Eq. (4.7), was introduced into Eq. (4.10). A plot of the error induced in the frequency-averaged turbulent intensity is shown in Fig. 12.

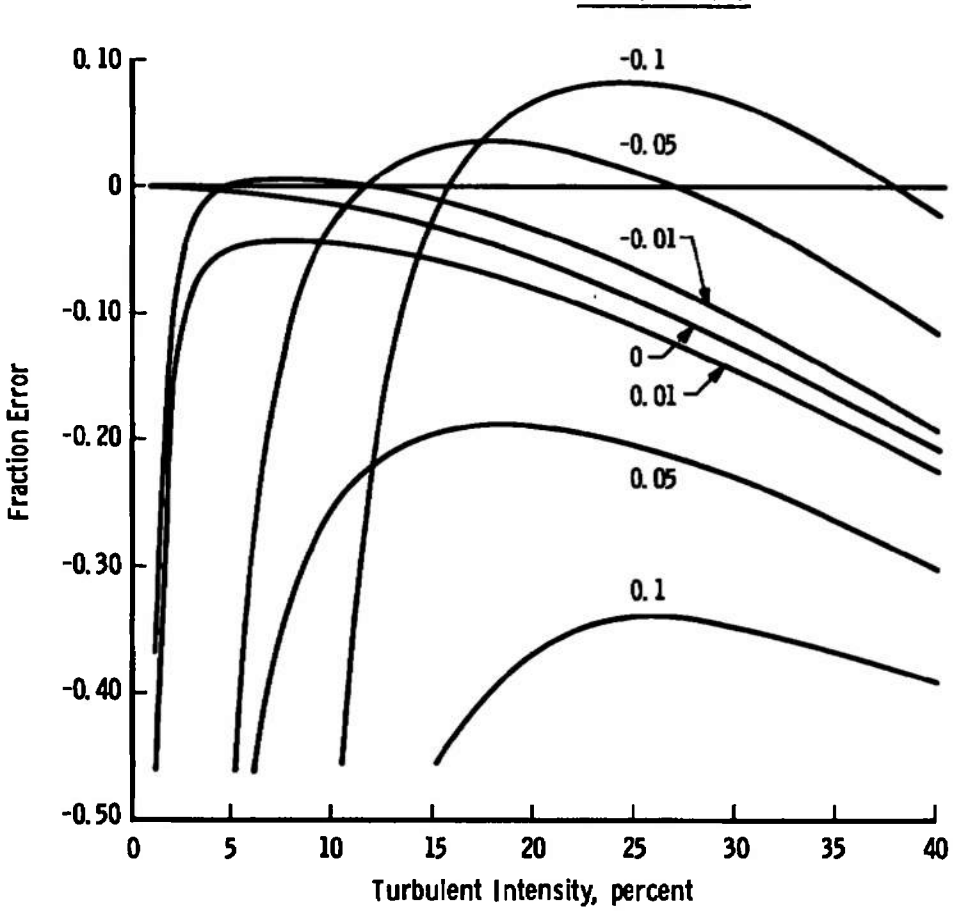

Figure 12. Fraction error in measured frequency-averaged turbulent intensity with $\langle n'v' \rangle / \bar{n}\bar{v}$ as a parameter.

The mean square of the period fluctuations is now calculated. Strictly speaking, this is not a velocity turbulent intensity. However, it does provide an estimator for the dimensionless turbulent intensity, which can be obtained both theoretically and experimentally.

$$\overline{(Tl)}^2_{mT} = \frac{\langle T'^2 \rangle_{mT}}{\bar{T}^2_{mT}} = \frac{\langle \dot{N}(T - T_{mT})^2 \rangle}{\dot{N}\,\bar{T}^2_{mT}} = \frac{\langle \dot{N} T^2 \rangle}{\dot{N}\,\bar{T}^2_{mT}} - 1$$

$$= \frac{\left\langle \frac{(\bar{n} + n')}{1 + \frac{v'}{\bar{v}}} \right\rangle \bar{v}^2_{mT}}{\bar{n}\bar{v}^2 \left(1 + \frac{\langle n'v' \rangle}{\bar{n}\bar{v}}\right)} - 1 \qquad (4.12)$$

Expanding $1/(1 + \frac{v'}{\bar{v}})$ into a series, substituting for $\bar{v}_{mT}$ and keeping only second-order terms, then

$$\overline{(TI)^2_{mT}} \cong \frac{\langle v'^2 \rangle}{\bar{v}^2}\left(1 + \frac{\langle n'v' \rangle}{\bar{n}\,\bar{v}}\right) - \left(\frac{\langle n'v' \rangle}{\bar{n}\,\bar{v}}\right)^2$$

The fraction error as a function of turbulent intensity is plotted in Fig. 13. Assuming the correlation between particle and velocity fluctuations is negligible, then

$$\overline{(TI)^2_{mT}} = \frac{\langle v'^2 \rangle}{\bar{v}^2}$$

Again, as with the mean velocity, period averaging leads to an unbiased estimate.

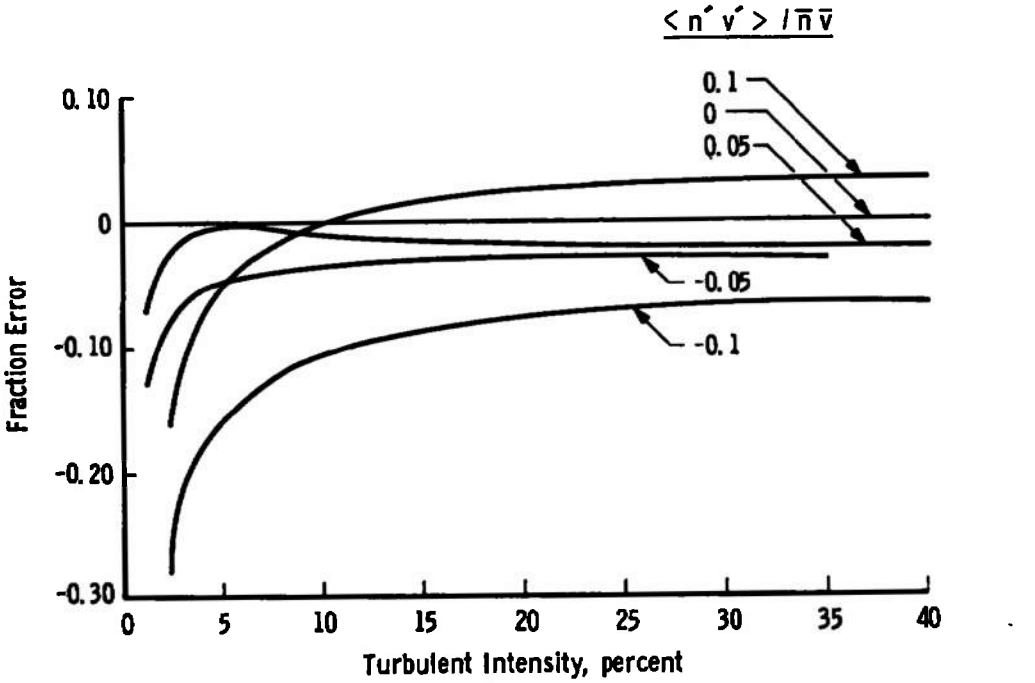

Figure 13. Fraction error in measured period-averaged turbulent intensity with $\langle n'v' \rangle / \bar{n}\,\bar{v}$ as a parameter.

The equations for the mean velocity and turbulent intensity estimators can be used to obtain the true mean velocity, turbulent intensity, and velocity-density correlation. Starting with Eqs. (4.11) and (4.13) and solving for $\langle n'v' \rangle / \bar{n}\,\bar{v}$ leads to a quartic equation. Only one of the roots leads to a physically meaningful solution. The corresponding turbulent

intensity and the velocity density correlation, when substituted into the equations for the mean velocity, Eqs. (4.7) and (4.9), should yield the same true velocity.

Figure 14 shows the true turbulent intensity as a function of the period- and frequency-averaged turbulent intensity. From an experimentally determined pair of turbulent intensity estimators the true turbulent intensity can be determined. Similarly, the velocity-density correlation has been determined and plotted in Fig. 15. Some care should be taken when the theory is applied to specific problems, as the assumptions are somewhat restrictive. Data should also be free of any other broadening or biasing effects which may be encountered in LV systems, such as noise-induced counts. Again, the theory outlined is valid only for data rates which are controlled by the particle arrival rates rather than by the processor dead time, and are high with respect to the velocity fluctuations.

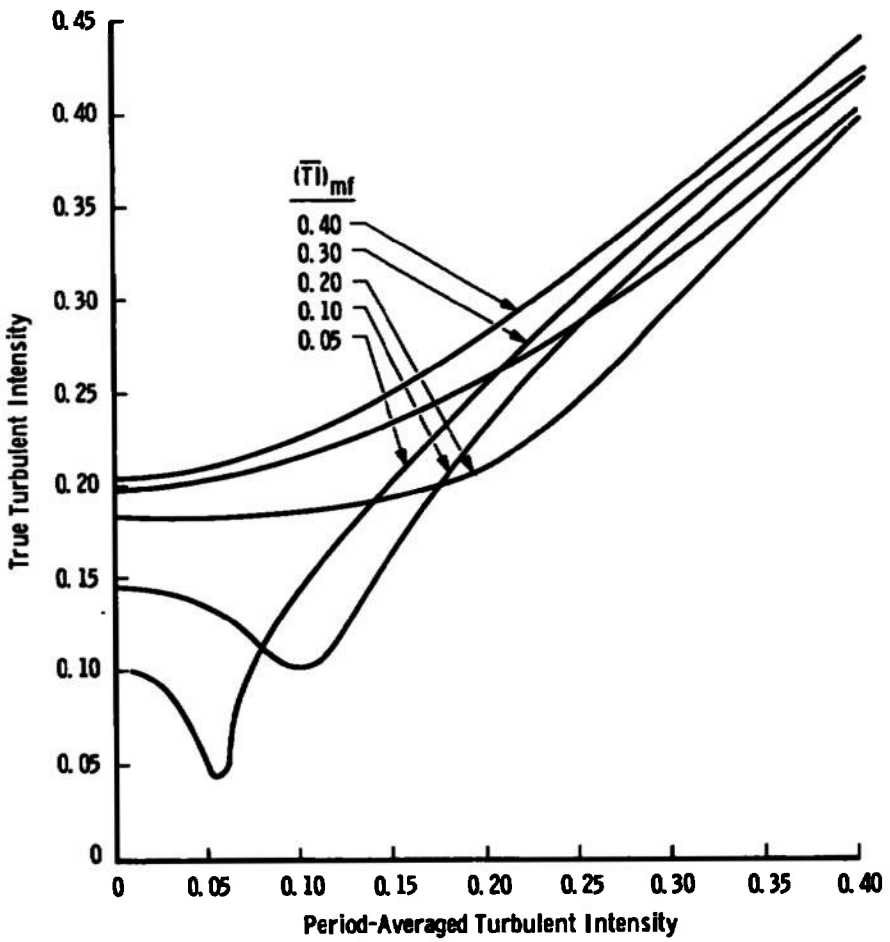

Figure 14. True turbulent intensity as a function of period- and frequency-averaged turbulent intensity.

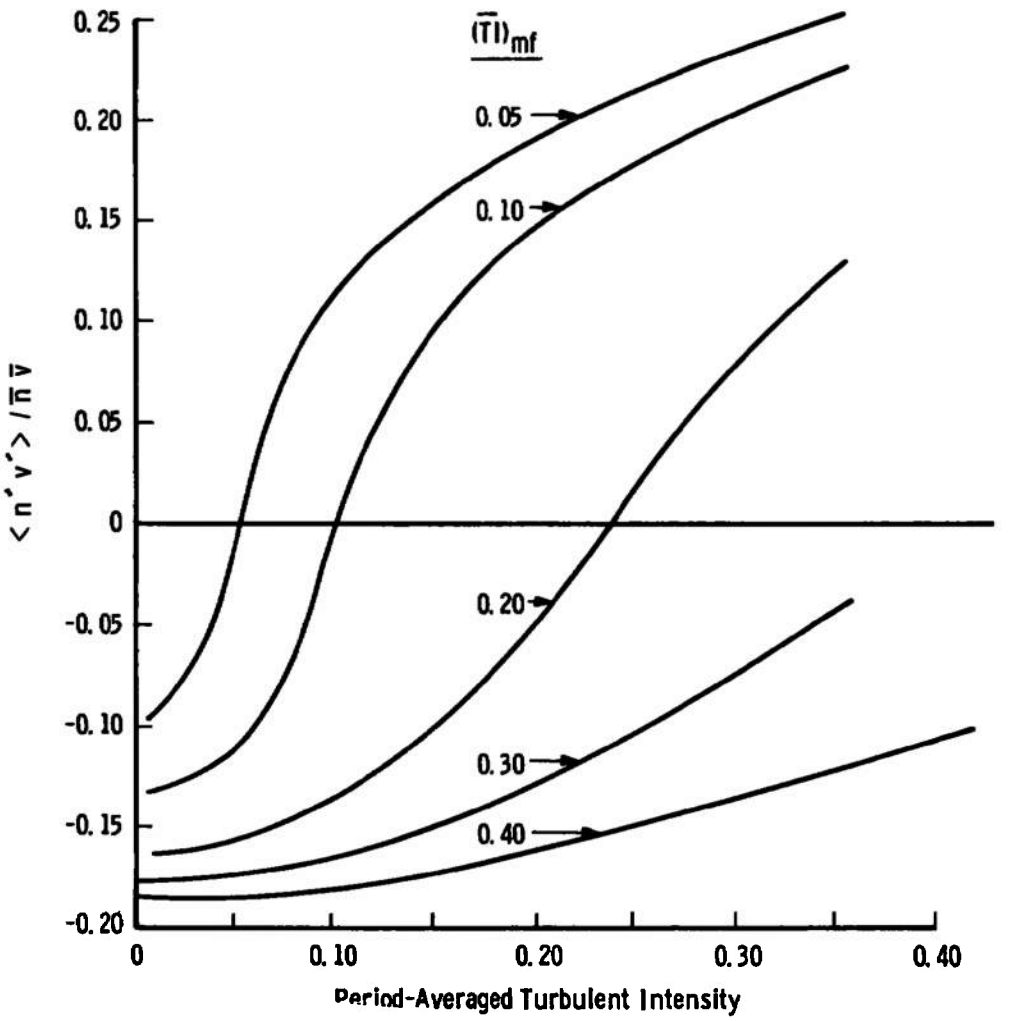

Figure 15. $\langle n'v' \rangle / \bar{n}\,\bar{v}$ as a function of period- and frequency-averaged turbulent intensity.

5.0 EXPERIMENTAL DATA

Laser velocimeter data were taken in a free-jet-mixing facility* to obtain mean velocity, relative turbulent intensity, and mean flow angularity. Hot-wire anemometer measurements were scheduled under another project for correlation purposes, but that phase of the project was not accomplished. Although there is no basis for comparison of the LV data, it is deemed useful in demonstrating the technique and will be briefly presented.

*Facility operation, along with pitot probe and hot wire measurements, was accomplished by personnel of the Engine Test Facility Fluid Dynamics and Propulsion Group in Research Test Cell R1A1.

The experiment comprised two concentric nozzles arranged as shown in Fig. 16. The plenum pressures were set to give a nominal 2:1 inner core to outer core velocity ratio, and the mixing of the jet exhausts formed the turbulent field.

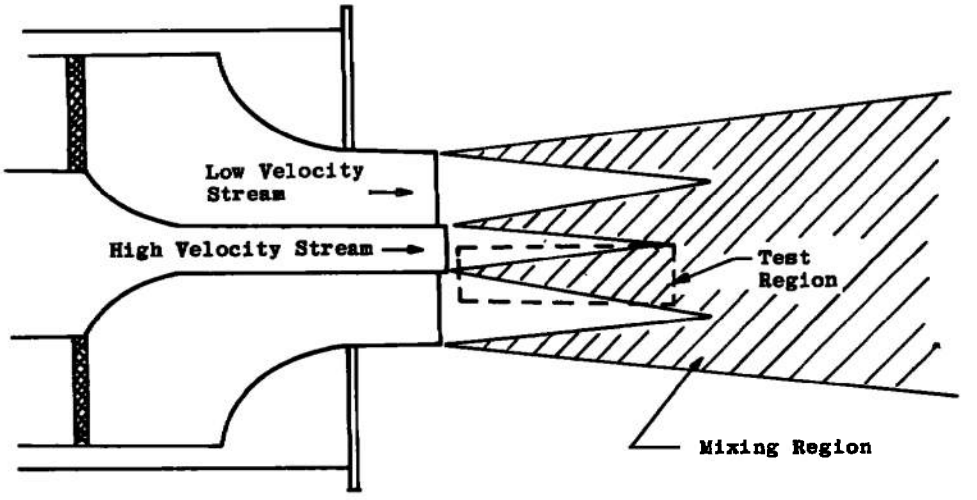

Figure 16. Free-jet-mixing configuration.

The LV was a dual scatter system operated in the forward scatter collection mode. It was set up to measure either of two velocity components, one at 33.7 deg. above horizontal and the other at 42.4 deg. below. The components were not measured simultaneously because of limited equipment, but were taken alternately at each location. This should have no effect on the data since the mean velocity and turbulent intensity level must be considered constant. At a rate of six data points per second, a 16-sec period (long with respect to typical flow variations) is required to acquire 100 data points. This count rate is much less than the rate of flow-field fluctuations.

The system was mounted on a traverse which scanned radially downward from centerline. Radial profiles were taken at five axial stations.

One hundred data bursts were processed for each component at each location. Under the assumptions of a normal distribution and a 10-percent turbulent intensity this would have assured (with 95-percent confidence) a sample mean velocity within at least 2 percent of true, and the turbulent intensity would not be off more than 16 percent (see Figs. 4 and 5).

The data were first reduced to show mean velocity and standard deviation for each velocity component.

$$\underline{\bar{v}} = \frac{\sum_{i=1}^{N} v_i}{N} \qquad \underline{\sigma} = \left[\frac{\sum_{i=1}^{N} (v_i - \bar{v})^2}{N - 1}\right]^{1/2}$$

The two velocity components were then resolved into the mean velocity vector ($\hat{V}$), the magnitude of which is

$$|\vec{V}| = \frac{v_1}{(\cos\theta_1 \cos\alpha + \sin\theta_1 \sin\alpha)}$$

where

$$\alpha = \tan^{-1}\left[\frac{v_2 \cos\theta_1 - v_1 \cos\theta_2}{v_1 \sin\theta_2 - v_2 \sin\theta_1}\right]$$

(The angles θ_1 and θ_2 are the angles of the measured components above and below earth horizontal, respectively.)

The relative turbulent intensity was then calculated in the direction of the measured components:

$$TI = \sigma_1/|\vec{V}| \quad \text{and} \quad \sigma_2/|\vec{V}|$$

These data are presented for three axial stations in Fig. 17. The turbulence appears to be nearly isotropic in the laminar region of the center flow, but definitely not in the mixing region, where $\sigma_2/|\vec{V}|$ is twice $\sigma_1/|\vec{V}|$ at one point. With no supporting data showing the shape of the turbulence envelope, no attempt was made to adjust the data to the flow coordinate system.

The data appear to be internally consistent. The spreading of the mixing region, as well as the decrease in peak intensity, is seen at successive downstream stations. It is seen that the peak occurs near the middle of the mixing region. The extreme values, between 2 and 20 percent, appear reasonable. Finally, the data, especially near centerline at X = 3 in. (Fig. 17a), show a smooth, fairly constant curve in that region.

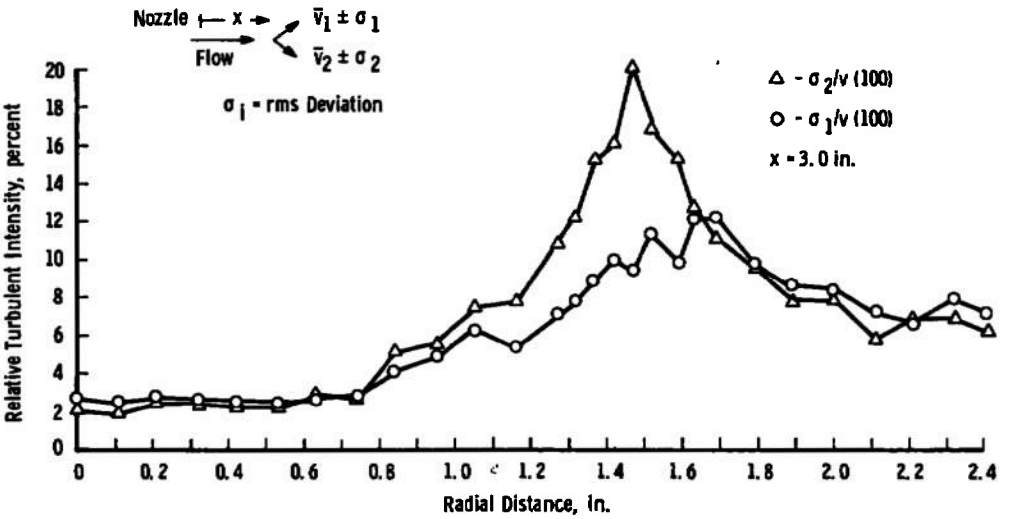

a. Axial distance = 3 in. from nozzle exit

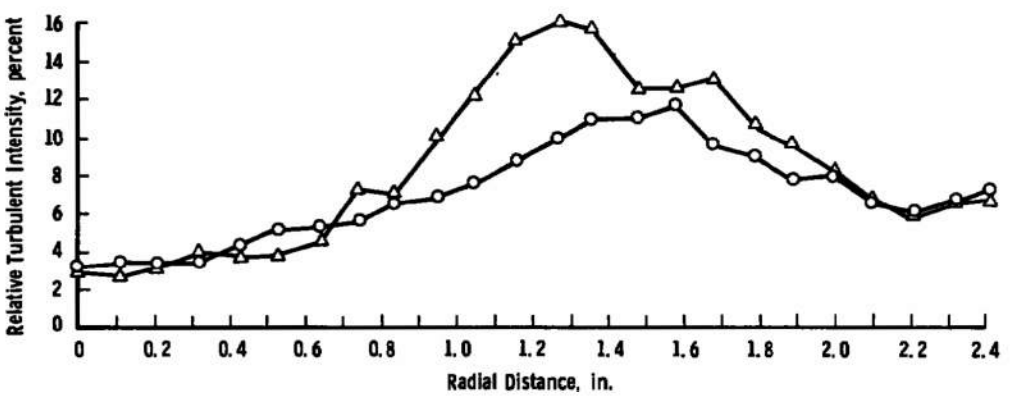

b. Axial distance = 6 in. from nozzle exit

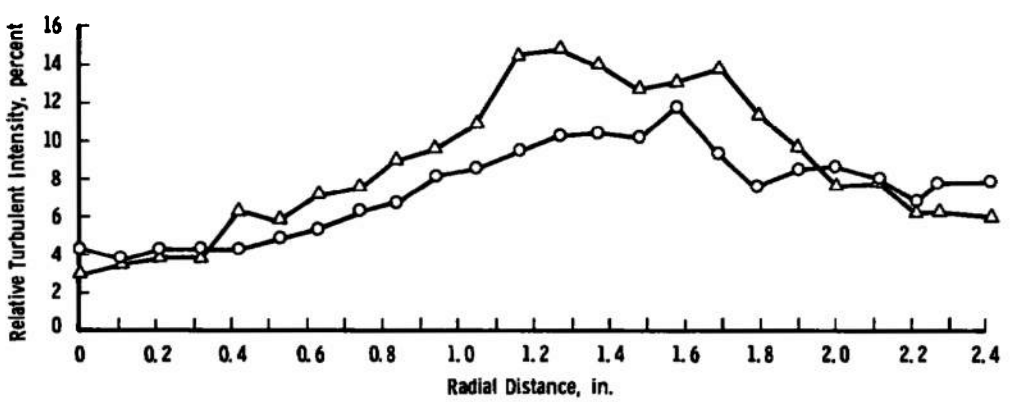

c. Axial distance = 9 in. from nozzle exit

Figure 17. Relative turbulent intensity profiles.

Hot-wire measurements of TI made for probe shakedown purposes were accomplished in nominally the same flow configuration (2:1 ratio) as the LV measurements. They were limited to two locations and were oriented in a different coordinate system; however, their values are of interest for general comparison with the LV data shown in Fig. 17. On centerline near the nozzle exit a value of 3 percent for the turbulent intensity was obtained with the hot wire in the 200 ft/sec flow. This agrees well with data on one LV component taken on centerline at each of the three axial stations shown. The other value, 13 percent, was obtained in the center of the mixing region. These data fall between those of the two LV components in all cases in that region.

The total relative turbulent intensity is given as

$$(\text{Rel. TI}) = \frac{\left(\sigma_1^2 + \sigma_2^2 + \sigma_3^2\right)/3}{|\hat{V}|}$$

where the subscripts indicate the three orthogonal directions in the flow coordinate system. For the purpose of calculating this property, it was assumed that the unmeasured third component (σ_3) was equal to the smaller of the other two. In this case there may be a basis for assuming that it is even much smaller since the azimuthal velocity should be very small and the energy gradient is radial. The absolute lower limit, where $\sigma_3 = 0$, and an upper reference, where $\sigma_3 = (\sigma_1 + \sigma_2)/2$, are shown with these data in Fig. 18 along with the mean velocity profile and the mean flow angularity. Again the 3 percent on the centerline and 13 percent in the mixing region from the hot wire compare well.

The mean flow angularity is referenced to earth horizontal. It appears that the inner core jet was about 0.5 deg above horizontal. An outward flow is indicated as the angle becomes more negative, corresponding to the radius at which the velocity begins to decrease, i.e., at the edge of the mixing region. In the outer half of the mixing region the mean flow angle is radially inward. Near-horizontal flow is again seen in the low velocity outer jet.

Pitot probe measurements of velocity were made concurrently with the LV measurements. The LV measurements were made upstream of the pitot probe to prevent interference. The two systems were mounted on separate traverse systems, and it was evident that the flow centerline determination was different for the two. Although the centerline determination for the pitot data was more accurate, the pitot data were arbitrarily made to coincide in radius with the LV data for this presentation.

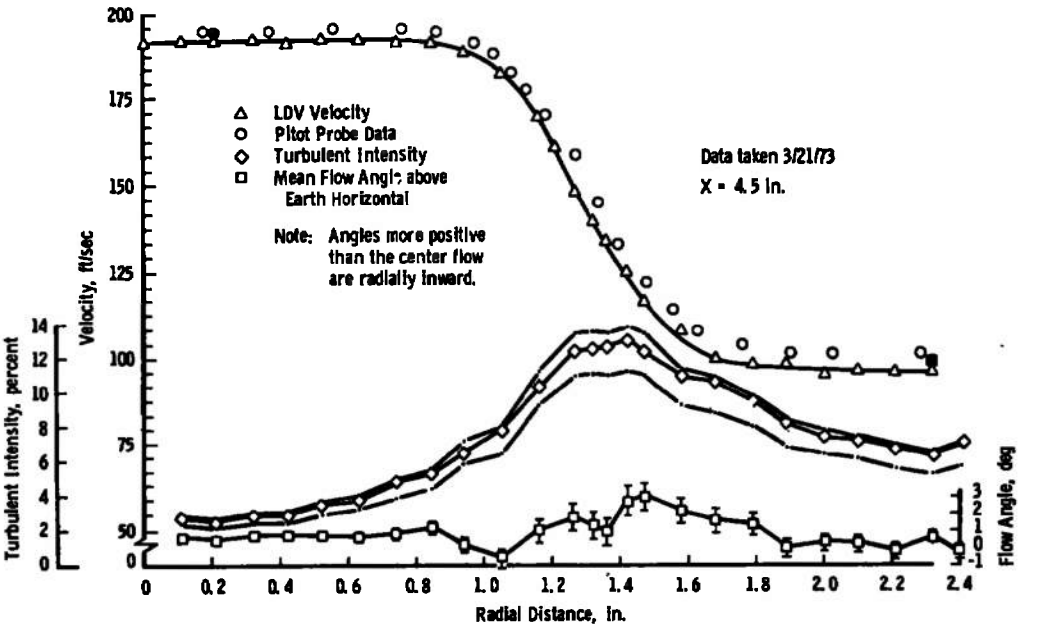

Figure 18. Velocity and turbulent intensity profiles from LDV data showing flow angularity.

A moderate discrepancy (from 4 to 5 percent) between the data of the two systems is evident. The discrepancy is believed to be caused by the data reduction technique used on the LV data. Unfortunately, the proposed new technique requires more data points than were taken; thus post-facto correction is impossible. Two points on the profile lent themselves to the new technique. They are shown in blackened symbols in in the figure, giving 0.3-percent agreement in the center flow and about 2-percent agreement in the low velocity region.

6.0 INSTRUMENTAL DATA BROADENING

The measured distribution is a convolution of the actual distribution of velocities in the flow and that of any broadening effects of the system. Two known systematic effects were investigated and found to be negligible.

There is a slight variation in fringe spacing on the outer extremes of the beam crossover region in a dual scatter system. This is due to the Gaussian intensity cross section of the interfering beams. For typical beam intersection angles it is on the order of 0.1 percent and is eliminated completely with an off-axis collection system since the questionable region is not seen by the collector lens system. (See typical probe volume in Refs. 10 and 11.)

It was also suspected that a distribution of measurements taken in a low signal-to-noise ratio (S/N) environment would be broadened by the noise pulses riding on the signal. This possibility was investigated experimentally using a white noise generator (a high gain amplifier), along with the LV Frequency Burst Signal Synthesizer, and the LV Data Processor, both described in Ref. 5. The noise signal was superimposed on the synthesized LV signal before it entered the data processor. A signal-to-noise rms power ratio was used. The rms signal amplitude was measured on an oscilloscope, and the noise amplitude was measured with a broadband rms voltmeter to set a given S/N. A constant signal frequency of 100 KHz was used to give a basic period of 10 μsec. A collection of at least 100 data points was recorded from the processor for each condition. The mean period ($\bar{\tau}$) and the relative deviation ($\sigma/\bar{\tau}$) were calculated. The data, presented in Table 1, show a dependence on both S/N and signal amplitude for the relative deviation. In the absolute extreme of poor S/N, 0.024, the relative deviation is on the order of 0.5 percent.

The variance of a measured velocity distribution σ_m^2 is related to the actual velocity distribution (σ^2) by $\sigma_m^2 = \sigma^2 + \sigma_n^2$ where σ_n^2 is the variance of the noise distribution; therefore,

$$\sigma = \left(\sigma_m^2 - \sigma_n^2\right)^{1/2}$$

Table 1. Data Broadening Due to Noise

S/N (Power Ratio)	Signal Amplitude, MV	Noise Amplitude, MV	Period-Averaged $\bar{\tau}$, μsec	$\sigma/\bar{\tau}$, percent
1:1	7.0	7.0	10.045	0.09
1:1	3.5	3.5	10.078	0.11
1:1	1.75	1.75	10.143	0.39
0.2	7.0	15.0	10.043	0.12
0.2	3.5	7.5	10.082	0.14
0.2	1.75	3.75	10.164	0.33
0.024	7.0	42.0	10.074	0.48
0.024	3.5	21.0	10.077	0.25
0.024	1.75	11.0	10.151	0.56

Assume the extremely poor conditions of S/N = 0.2 and signal amplitude = 1.75 mv, which would give σ_n = 0.33 percent. Assume also a reasonable minimum measured deviation, σ_m = 3.0 percent. For this "worst case" condition, σ would be 2.98 percent for a 0.67-percent error in the measured value. A well designed LV should exceed a S/N of unity and a 7-MV signal amplitude, whereby the measured deviation error should be less than 0.06 percent. This is not a significant contribution to the turbulent intensity measurement.

7.0 SUMMARY AND CONCLUSIONS

The LV system is well suited for direct measurements of turbulent intensity. All of the systematic broadening effects are insignificant with respect to typical flow turbulent intensities of 3 percent and above.

It was found that a much larger quantity of data than previously expected is required to specify a given accuracy on a measurement of TI. This is true because the typical data obtained were not normally distributed and exhibited large values for the kurtosis. The analytical relationship defining required sample size was verified for large N values by two sets of experimental data. It has been shown that the kurtosis is affected slightly by the turbulence source. If it can feasibly vary widely, then an estimate of kurtosis will be needed before an estimate of sample size can be made for each location in a turbulent field. The other alternative would be to use a pessimistic value of kurtosis and accept the resulting tolerance on the measurements.

Indications are that kurtosis is more affected by other system or flow characteristics such as large particle dynamics, which could cause a variation in the low velocity tail of the distribution. If this is the case, it may be possible to discriminate against such data points by flow filtering or electronic means, and to decrease the required sample size. Further studies are needed in this area defining the significant effects on the characteristics of the measured distribution.

It was found that both frequency averaging and period averaging presented a biased estimator of TI and $\bar{\bar{V}}$. The system of equations developed to predict the biases forms a basis for generalization to more complex geometries. The period-averaged mean velocity, in general, is least biased and is independent of turbulent intensity, when sample rates are very high. However, for most practical applications this bias is small, as sample rates are controlled by instrument deadtime.

REFERENCES

1. Dunning, John W., Jr. and Berman, N. S. "Turbulence Measurements Using the Laser Doppler Velocimeter." Project SQUID, Workshop Proceedings, Purdue University, March 9-10, 1972.
2. Mayo, W. T., Jr., Shay, M. T., and Riter, S. "The Development of New Digital Data Processing Techniques for Turbulence Measurements with a Laser Velocimeter." AEDC-TR-74-53, August 1974.
3. Asher, J. A., Scott, P. F., and Wang, J. C. "Parameters Affecting Laser Velocimeter Turbulence Power Spectra Measurements." AEDC-TR-74-54 (To Be Published).
4. Lennert, A. E., Brayton, D. B., Crosswy, F. L., et al. "Summary Report of the Development of a Laser Velocimeter to Be Used in AEDC Wind Tunnels." AEDC-TR-70-101 (AD871321), July 1970.
5. Kalb, H. T., Brayton, D. B., and McClure, J. A. "Laser Velocimetry Data Processing." AEDC-TR-73-116 (AD766418), September 1973.
6. Laufer, J. "Investigation of Turbulent Flow in a Two-Dimensional Channel." NACA Rept. 1053, 1951.
7. Hansen, M. H., Hurwitz, W. N., and Madow, W. G. Sample Survey Methods and Theory. Vol. II. John Wiley and Sons, Inc., New York, 1960.
8. Yanta, W. J. "Turbulence Measurements with a Laser Doppler Velocimeter." NOL-TR-73-94, May 1973.
9. Barnett, D. O. and Bentley, H. T., III. "Statistical Bias of Individual Realization Laser Velocimeter Systems." Proceedings of the 2nd International Workshop on Laser Velocimetry, March 27-29, 1974, Purdue University, Lafayette, Indiana (To Be Published).
10. Brayton, D. B., Kalb, H. T., and Crosswy, F. L. "Two-Component Dual-Scatter Laser Doppler Velocimeter with Frequency Burst Signal Readout." Applied Optics, Vol. 12, June 1973.
11. Cline, V. A. "Dust Particle Velocity Measurements Using a Laser Velocimeter." AEDC-TR-72-159 (AD752225), December 1972.

APPENDIX A
BIAS EFFECTS OF INDIVIDUAL REALIZATION VELOCIMETERS,
by D. O. Barnett

The turbulence at a point in an incompressible, isothermal flow can be totally characterized if the velocity history, V(t), is known. In LV practice, however, only certain velocity moments are obtained which, together with basic assumptions concerning the velocity distributions, adequately describe the process of interest.

If $Q = Q(V)$, then the quantity one wishes to approximate with an LV system is the temporal mean of Q, which may be defined as follows:

$$\langle Q \rangle = \frac{1}{T} \int_0^T Q(V)dt \tag{A-1}$$

Data taken with an individual realization LV are not continuous, and consequently Eq. (A-1) must be approximated as

$$\{Q\} = \frac{1}{T} \sum_{i=1}^{M} Q_i \Delta t_i \tag{A-2}$$

where $\{Q\}$ is now an estimator for $\langle Q \rangle$, the desired temporal average of Q.

While the individual Q_i values are accurately known, the corresponding sample intervals, which minimize bias, require a general model of the sampling process. Obviously a deterministic prediction of the exact arrival times at the probe volume cannot be made. However, if in the vicinity of the probe volume the number density is constant, then the time interval between successive samples for one-dimensional flow can be written as

$$\Delta t_i = \frac{1}{\langle V_i \rangle} \times \frac{1}{nA} \tag{A-3}$$

where $\langle V_i \rangle$ is the time-averaged fluid velocity over the interval, n is the particle number density, and A is the probe area. Correlations between the velocity and particle density have not been included, but it should be noted that Eq. (A-3) implies that there is a strong correlation between velocity changes in the probe volume and the velocity immediately upstream of the probe volume.

Upon introduction of Eq. (A-3) into Eq. (A-2) and noting that

$$T = \sum_{i=1}^{M} \Delta t_i \tag{A-4}$$

one solves for the temporal mean of Q thus:

$$\{Q\} = \frac{\sum_{i=1}^{M} Q_i / \langle V \rangle_i}{\sum_{i=1}^{M} 1/\langle V \rangle_i} \tag{A-5}$$

The conditions under which Eq. (A-5) yields an unbiased estimate of $\langle Q \rangle$ will now be determined.

Expanding V(t) in a series of the form

$$V(t) = \langle V \rangle + \sum_{N=1}^{\infty} V_N \cos(\omega_N t - B_N) \tag{A-6}$$

yields an expression which is valid over the entire sampling time, T. By integration (Eq. A-6) over a sample interval Δt_i, the mean value can be obtained.

$$\langle V \rangle_i = \langle V \rangle + \sum_{N=1}^{\infty} V_N' \sin(\omega_N t_i - B_N) \left(\frac{\cos \omega_N t_i - 1}{\omega_N \Delta t_i} \right) \tag{A-7}$$

Case I: Sample Frequency Less Than Minimum Flow Frequency.

When $\omega_N \Delta t_i \gg 1$ (that is, when the sampling frequency is much less than the lowest frequency of the flow oscillations of interest), $\langle V \rangle_i \rightarrow \langle V \rangle$. For this case the time interval of the sample is essentially constant, and the temporal of Eq. (A-5) and the arithmetic average are identical. The arithmetic average is defined as

$$\overline{Q} = 1/M \sum_{i=1}^{M} Q_i \tag{A-8}$$

It follows that the mean velocity over the entire time interval, T, also is given by the arithmetic mean of the sample velocities, V_i. While this procedure does not prove the equivalence of the arithmetic and temporal averages, it should be noted that for sample frequency low

with respect to the minimum significant frequency component, any correlation between the instantaneous velocity and the sampling rate tends to be destroyed. Since it is equally probable that during any sample interval the sampled velocity will be greater or less than the mean value, the arithmetic mean should provide an unbiased estimator of the mean velocity.

Case II: Sample Frequency Greater Than the Maximum Flow Frequency

If the sample frequency is large compared to the frequency of the flow oscillations, then $\omega_N \Delta t_i << 1$.

For this case, the individual sample accurately represents the velocity during the time interval. In essence, the flow appears stationary during the sample interval, and $\langle V \rangle_i \cong V_i$. Furthermore, for large sample sizes the finite sum, Eq. (A-2), becomes an excellent approximation to the temporal mean, Eq. (A-1). Equation (A-2) reduces to the harmonic average of the individual realizations of the velocity thus:

$$\{V\} = \frac{1}{\frac{1}{M}\sum_{i=1}^{M} 1/V_i} = \frac{K}{\bar{\tau}} \tag{A-9}$$

where K is a constant (a function of the LV geometry and wavelength), and the period is given by $\tau_i = 1/f_i$.

It is thus Eq. (A-8) which forms the basis for the statistical bias of the LV data. The interpretation of the harmonic-averaged velocity data as a "period-averaged" velocity is evident.

One can show that the arithmetic average of the frequency yields higher mean values than the harmonic-averaged result. This may be demonstrated by letting

$$f_i = \bar{f} + f_i' \tag{A-10}$$

Upon substituting into the expression for the harmonic mean, Eq. (A-8), and using the expansion for $(1 + x)^{-1}$,

$$\bar{V} = k\bar{f} = \{V\} \sum_{r=0}^{\infty} (-1)^r \overline{f'^r}/\bar{f}^r \tag{A-11}$$

for $f' < \bar{f}$. For symmetric velocity distributions and, hence, frequency distributions, the odd order moments (i.e., r = 1, 3, 5 . . .) yield

vanishing central moments, establishing the inequality of the arithmetic and temporal averages.

The analysis indicates that for one-dimensional flow through the probe volume of an LV system, it is possible to obtain arithmetic averages which are biased with respect to the temporal mean velocity of the fluid. If the sampling frequency is much higher than the frequency of the velocity fluctuations, the bias can be as large as predicted by the analysis. On the other hand, sampling at low frequency will eliminate the fundamental bias. The situation, however, will be mixed in turbulent flow where many harmonics will occur.

For those sample rates where bias is predicted, the bias in the mean velocity can be eliminated by harmonic averaging of the individual realizations of velocity.